Porous nanostructured layers on germanium produced by Laser optical breakdown processing

A. V. Kabashin*, V-G. Pilon Marien, D.-Q. Yang, F. Magny, and M. Meunier
Laser Processing Laboratory, Ecole Polytechnique de Montréal, Case Postale 6079, Succ. Centre-ville, Montréal (Québec), Canada, H3C 3A7

ABSTRACT

Germanium wafer surface is modified by a technique of CO_2-laser induced air breakdown processing, which was recently introduced and used to produce photoluminescent Si-based nanostructured layers. Structural and optical properties of the Ge-based layers, formed under the irradiation spot as a result of the processing, are characterized by different techniques (SEM, XPS, FTIR, XRD, and PL). It has been found that the layers present a porous structure, containing nanoscale holes, and consist of Ge nanocrystals embedded into GeO_2 matrices. They exhibited strong photoluminescence (PL) in the green range (2.2 eV), which was attributed to defects in GeO_2 matrix due to the presence of Ge-O modes with some OH vibration in the FTIR spectra. The layers are of importance for local patterning of nanostructures on semiconductors.

Keywords: air optical breakdown, nanostructured Ge, visible photoluminescence, laser-assisted patterning

1. INTRODUCTION

Silicon and Germanium are group IV semiconductors, which are of vital importance for the microelectronics industry. However, having indirect and small band gaps (1.1 eV for Si and 0.6 eV for Ge), both materials do not emit visible light, which complicates their use for optoelectronics applications. Novel promises for these applications arose with the observation of visible photoluminescence (PL) from anodically etched porous Si[1] and nanostructured thin films prepared by different "dry" deposition techniques.[2-8] Similar effect was observed with chemically etched Ge[9,10] and Ge-based films[11-13]. Even if the origin of visible PL has not yet been clarified, applications of nanostructured semiconductors in photonics[14] and biosensing[15] are now extensively discussed.

By now there is a significant interest in the development of methods for local patterning of the nanostructured layers on a semiconductor wafer and, potentially, on an assembled integrated chip or optoelectronics device. One of the simplest vacuum-free and "dry" methods for the local nanostructuring is the processing of a semiconductor wafer by an electric spark[16-20]. The wafer is used as a cathode in a plasma-assisted process, in which unipolar discharges between two electrodes ionize the gaseous environment and accelerate the generated ions toward the semiconductor surface leading to its structural modifications. In the case of Si, the processed material exhibits PL with peaks in red (1.9 eV), green (2.36 eV) and UV/blue (3.22 eV) spectral ranges at room temperature[19]. In contrast, spark-processed germanium demonstrates a single PL peak at 2.2 eV.[20] Alternatively, we recently demonstrated another dry and vacuum-free method for local nanostructuring of semiconductors,[21,22] The method consists in the IR laser radiation-induced initiation of air breakdown on the semiconductor surface, while the target presence serves to decrease the threshold of the plasma initiation. The hot plasma of air optical breakdown causes a modification of target material, transforming it to a porous nanostructured layer. The method was successfully applied to treat silicon wafers and produce local nanostructured spots, exhibiting strong 1.9-2.0 PL.

* akabach@email.phys.polymtl.ca; phone 1-(514)340-4711 ext. 4634, Laser Processing Laboratory, Ecole Polytechnique de Montréal, Case Postale 6079, succ. Centre-ville, Montréal (Québec), Canada, H3C 3A7

In this paper, we apply the air optical breakdown technique to treat a germanium wafer and study properties of the layers formed on the wafer surface.

2. EXPERIMENTAL

In the experiments, the radiation from a pulsed TEA CO_2 laser (wavelength 10.6 μm, pulse energy 1 J, pulse length 1 μs FWHM, repetition rate 3 Hz), was focused by a Fresnel's lens (focal length of 5 cm) onto a Ge target. The radiation intensity was about 10^8 W/cm^2 at the focal plane. The experiment was carried out in atmospheric air (1 atm, 20° C, 40% humidity). Standard germanium wafers (n- and p-type, resistance 0.01- 10 Ohm·cm) with dimensions about 1×1 cm^2 were used as targets.

Scanning Electron Microscopy (Phillips XL20, Phillips Corp) was used to examine structural properties of the films. The crystalline structure of the films was examined by X-ray diffraction (XRD) spectroscopy (X'pert XRD system, Philips Corp). The surface analysis was performed at a base pressure below 10^{-10} Torr by the X-ray Spectroscopy (ESCALAB 3 Mark II, VG Scientific), using 1253.6 eV radiation from a Mg K_α X-ray source. High-resolution spectra were obtained at a perpendicular take-off angle, using 20 eV pass energy and 0.05 eV steps. Photoacoustic FTIR spectra were obtained using a He-purged MTEC 300 photoacoustic cell in a Bio-Rad FTS 3000 spectrometer[23]. The 2.5 kHz modulation frequency was used to probe the entire sample thickness. The PL spectra were measured at room temperature using a double spectrometer (model U100, Instruments SA) and a GaAs photomultiplier (Hamamatsu Photonics). The samples were illuminated by the radiation of a cw Ar^+ laser (model INNOVA 100) with the wavelength 488 nm.

3. RESULTS

3.1 Conditions of surface treatment

As in the case of silicon,[21,22] the breakdown initiation threshold on Ge depended on the efficiency of radiation absorption by the upper target surface layer. In particular, relatively high radiation powers were required to ignite the breakdown on a clean Ge wafer. However, the threshold was significantly lower when the radiation spot hit a dust on the wafer surface. After the breakdown ignition, the plasma intensity rose progressively with the number of laser shots on the same spot and stabilized only after 20-100 shots. The intensity gain was apparently related to the improvement of radiation absorption due to the formation of mechanical defects on the surface. In our experiments, the treatment was performed under near-threshold conditions to minimize possible deposition of material on the surrounding free target surface. After breakdown initiations by several laser pulses, a gray-tint area was formed under the focal spot on the silicon surface.

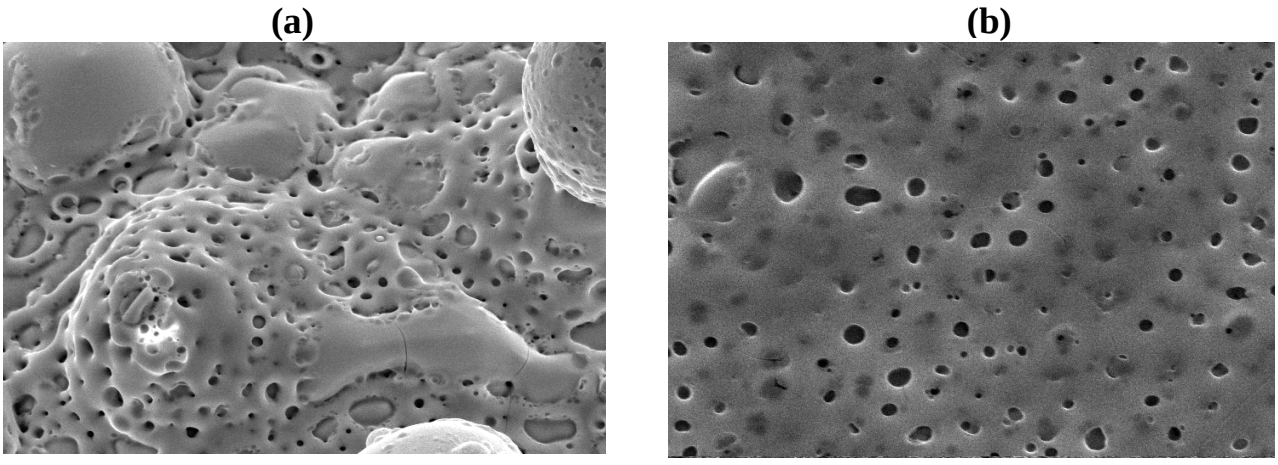

Fig. 1 SEM images of the treated Ge surface after 900 laser shots. (a) central region, 2000×, (b) peripheral region, 5000×

3.2 Surface morphology

It was found that the morphology of Ge surface after the laser irradiation was inhomogeneous. As one can see from SEM images depicted in Fig. 1, the processed layer was relatively non-uniform with casual formation of hill-like structures in the center of the irradiated spot, whereas in the peripheral part these structures were essentially absent. Nevertheless, the entire treated surface presented a highly porous material, containing nanoscale holes between 30 and 150 nm. It is worth mentioning that similar porous structures were observed after the air optical breakdown of silicon.

3.3 Surface chemical composition

We concluded from XPS spectra that only C, O and Ge were present in the surface modified layer of Ge. The peaks related to these elements can be clearly identified in the survey spectrum shown in Fig.2 (a). As follows from Fig. 2 (b), the high-resolution XPS spectrum of Ge samples before the treatment was characterized by peaks at 29 eV and 32.5 eV [Fig. 2 (b)], which are always assigned to the inoxidized Ge core and the natural GeO_2 oxide layer, respectively. Similar to the case of breakdown-treated Si[21,22], the treatment of Ge led to the disappearance of Ge-related peak, while the oxide-related peak became stronger, suggesting that the treatment led to a formation of germanium oxide shell (GeO_2). Thus, we can conclude that the upper treated layer mainly consisted of the germanium oxide.

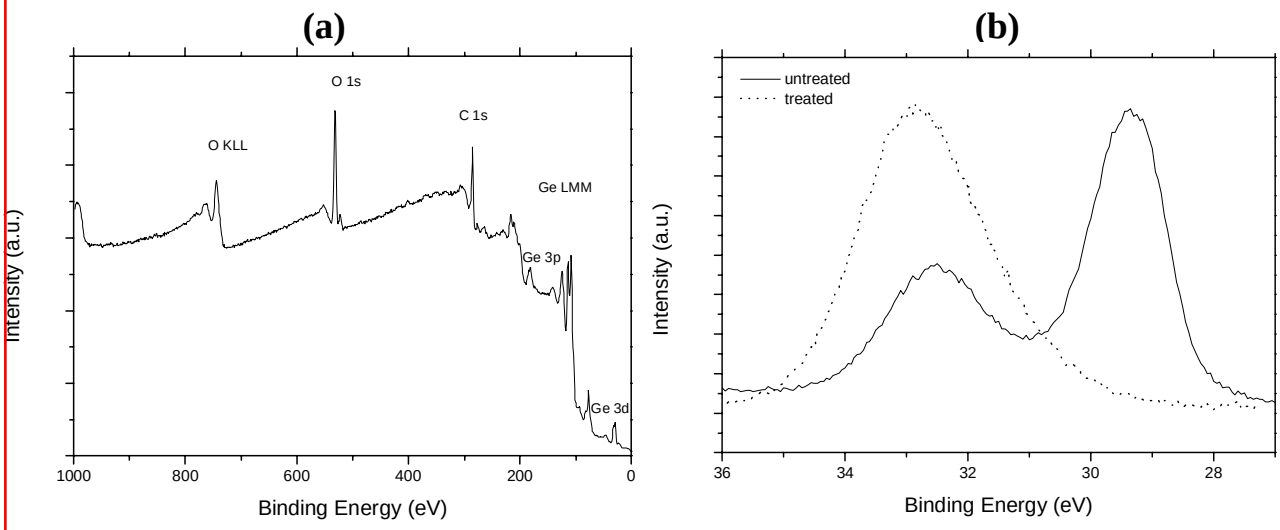

Fig. 2 XPS survey (a) and high-resolution (b) spectra from the breakdown-treated Ge surface after 900 pulses

Fig. 3 shows a typical photoacoustic FTIR spectrum from the treated surface. The major vibration features observed are the following: (a) The very strong and broad band, ~3500cm^{-1} , is assigned to bonded OH stretching vibration, while a sharp shoulder, appeared at ~3700 cm^{-1}, is usually assigned to the free absorbed OH; (b) ~2900 cm^{-1} band, which can be assigned to the C-H stretching mode associated with the CH_m groups adjacent to the OH groups; (c) ~1050 cm^{-1}, which can be attributed to Ge-O stretching, the C-O stretching mode and Ge-OH, as well as Ge-O-C stretching is also located in this region, (d) the CH_2 chain-wagging mode progression at 1200-1350 cm^{-1}, (e) the C-H scissors deformation mode of the CH_2 group ~1500 cm^{-1}. Disregarding signals related to carbon contamination of samples, we may conclude from the photoacoustic study that two types of important chemical processes occur during the treatment. These are the oxidation and formation of hydroxyl groups related to Ge-O and Ge-OH stretching modes, respectively.

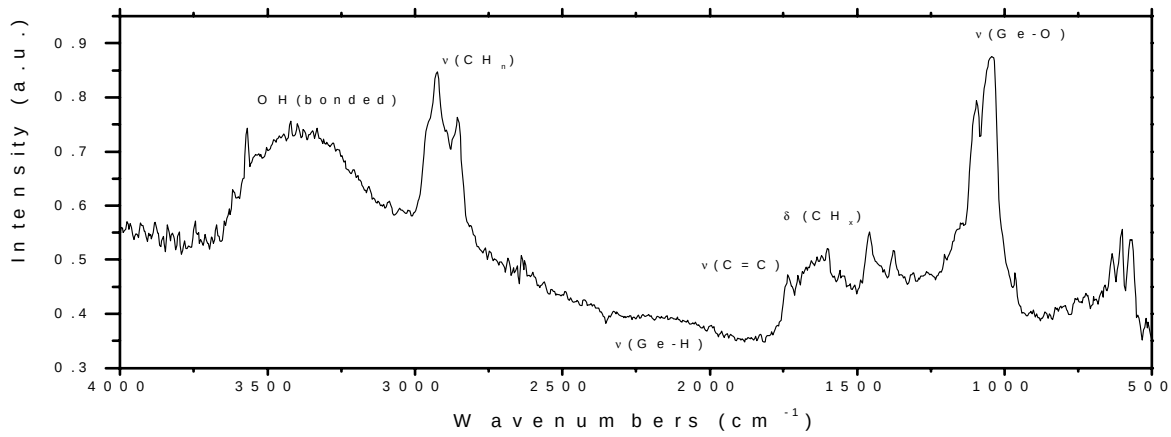

Fig. 3 Photoacoustic FTIR spectrum from the breakdown-processed Ge surface after 900 pulses.

3.4 XRD analysis

Nevertheless, XRD studies showed that Ge crystals are also present in the layer. Fig. 4 (a) shows typical spectra for a Ge target before and after the optical breakdown processing. One can see that the treatment led to the appearance of additional XRD peaks associated with different crystalline Ge states. This gives the evidence that the resulting layers consisted of Ge crystals embedded in GeO_2 matrix. It is known[24] that the broadness of XRD peaks is mainly determined by the smallest clusters in a deposit. As the instrumental noises are relatively low, this property could be used to roughly estimate the minimal size of crystals in the layer by the Debye-Scherrer formula[24]. Since the measured broadness of a typical Ge peak $\Delta(2\theta)/2$ is about 0.5 deg., the estimation gives the crystal size of the order of 20-30 nm. These values are similar to the nanocrystal size in the case of Si, obtained by the same method[21,22].

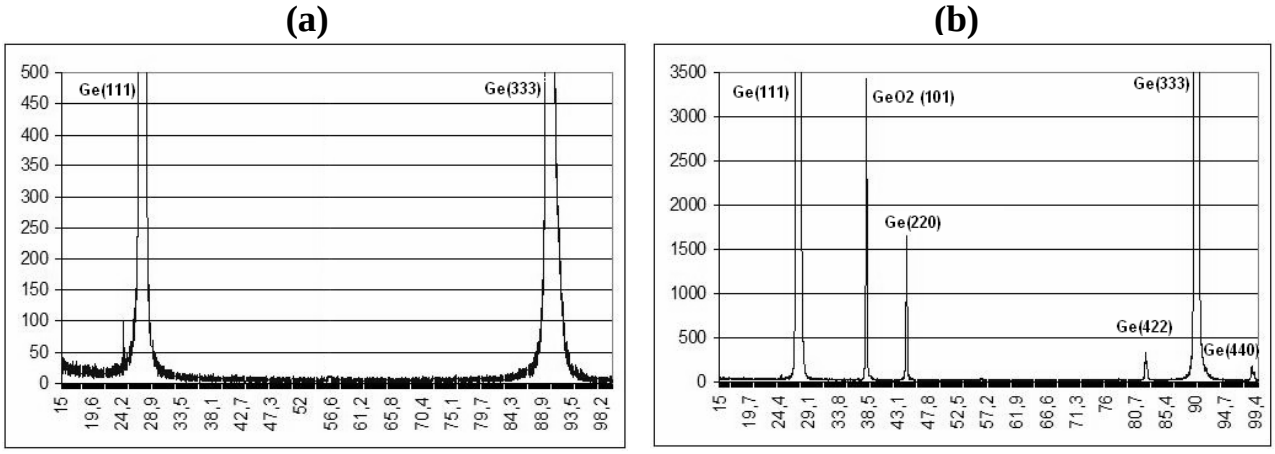

Fig. 4. Typical XRD spectra before (a) and after (b) the breakdown processing of a Ge wafer. To enhance XRD signal, a rectangular area with dimensions of 5×5 mm^2 was treated on the wafer by shifting the laser beam over the target.

3.5 PL studies

Similar to the case of Si, the breakdown-processed Ge surface shows strong visible PL in room temperature, which was visible by a naked eye. However, the maximum of PL emission was blue-shifted in comparison with Si (1.95 eV) and concentrated in the green range around 2.1-2.2 eV. As in the silicon case, the emission was uniform over the layer surface. It should be noted that similar PL signals were observed after the electric spark processing of germanium.[20]

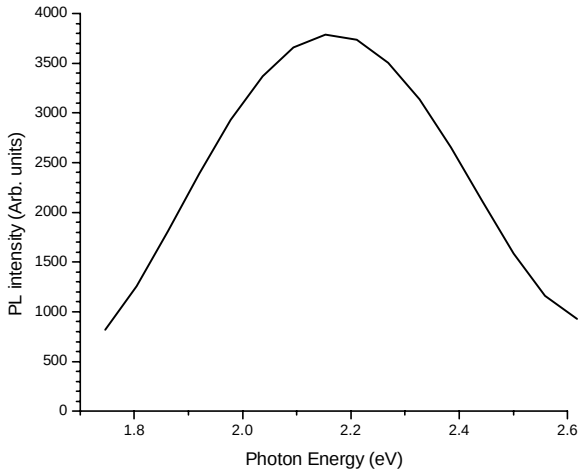

Fig. 5 Typical photoluminescence spectrum from the central part of Ge-based layer fabricated by the breakdown processing of a Ge wafer by 900 laser shots.

4. DISCUSSION

It is well known that the interaction of the CO_2 laser radiation with matter is characterized by a fast transition from a target-related to plasma-related radiation absorption[25]. The target generates initial electrons to ignite the gas discharge, which then develops in the cold gas toward the focusing lens, absorbing main IR radiation power and, as a consequence, getting heated up to high temperatures of more than 10^4 K.[25] The action of radiation probably causes a localized melting and even flash evaporation of the target material, leading to the appearance of pores on the target surface[22]. The laser-ablated material and the upper target layer are then heated by the hot CO_2 laser-induced breakdown plasma or its currents, leading to additional phase transformations and the initiation of chemical reactions. Since the radiation is pulsed, one can assume recrystallization or local vapor redeposition of the material during the off-times.

We believe that the mechanism of air optical breakdown processing is similar to the case of the electric spark processing[16-20]. Here, the modifications are attributed to pulsed ion bombardment of silicon surfaces, which led to a flash evaporation of the target material and its recrystallization during the off-times. Indeed, many properties of spark-processed and optical breakdown-processed semiconductors are similar. In particular, the spark-processed semiconductors also contained 10-500 nm holes and consisted of Si (Ge) nanocrystals embedded in SiO_2 (GeO_2) matrix[16,18,20]. Though PL properties of Si-based layers produced by these two methods could have certain differences, the Ge-based layers demonstrated similar properties with a strong peak at 2.1-2.2 eV. The generation of visible PL in the case of the spark-processed Ge was attributed to defects in GeO_2 structure rather than to the radiative recombination of excitons confined in nanocrystals[20]. In our opinion, this mechanism is also the most probable in the case of the optical breakdown processing. Indeed, plasma interaction with the Ge surface during the laser irradiation should form a large amount of defects in the oxidation layer and the interface. This is confirmed by the FTIR studies [Fig. 3], which gave a strong evidence for the OH absorption due the defect-related free radicals and dangling bonds. The quantum confinement effects are less probable in the case of Ge, but they can not be ruled out completely, taking into account that the nanocrystal size calculation by the Debye-Scherrer formula (in our case, 20-30 nm) is generally considered as a very rough estimation. In any case, more experimental data should be obtained for a clear identification of the PL origin. These studies are in progress.

5. CONCLUSION

Air optical breakdown has been produced on a Ge target to modify its surface. We showed that the breakdown production led to the formation of porous layer under the radiation spot, which consisted of Ge nanocrystals imbedded in GeO_2 matrix, while its surface was characterized by the presence of oxide and hydroxyl groups. The fabricated layers exhibited strong green PL, which is of importance for optoelectronics applications.

ACKNOWLEDGEMENTS

The authors are grateful to R. Leonelli for assistance during PL studies. We also acknowledge the financial contribution from the Natural Science and Engineering Research Council of Canada.

REFERENCES

1. L. T. Canham, "Silicon quantum wire array fabrication by electrochemical and chemical dissolution of wafers", *Appl. Phys. Lett.*, **57**, pp. 1046-1048, 1990.
2. H. Takagi, H. Ogawa, Y. Yamazaki, A. Ishizaki, and T. Nakagiri, "Quantum size effects on photoluminescence in ultrafine Si particles", *Appl. Phys. Lett.*, **56**, pp. 2379-2380, 1990.
3. Y. Kanemitsu, T. Ogawa, K. Shiraishi, and K. Takeda, Visible photoluminescence from oxidized Si nanometer-sized spheres: exciton confinement on a spherical shell", *Phys Rev. B*, **48**, pp. 4883-4886, 1993.
4. I. A. Movtchan, R. W. Dreyfus, W. Marine, M. Sentis, M. Autric, G. Le Lay and N. Merk, "Luminescence from a Si-SiO_x nanocluster-like structure prepared by laser ablation", *Thin Solid Films*, **255**, pp. 286-289, 1995.
5. Y. Yamada, T. Orii, I. Umezu, Sh. Takeyama, and T. Yoshida, "Optical properties of silicon nanocrystallites prepared by excimer laser ablation in inert gas", *Jpn. J. Appl. Phys., Part 1*, **35**, pp.1361-1365, 1996.
6. T. Makimura, Y. Kunii, and K. Murakami, "Light emission from nanometer-sized silicon particles fabricated by the laser ablation method", ", *Jpn. J. Appl. Phys., Part 1*, **35**, pp.4780-4784, 1996.
7. A.V. Kabashin, M. Meunier, and R. Leonelli, "Photoluminescence characterization of Si-based nanostructured films produced by laser ablation", *J. Vac. Sci. Tech. B*, **19**, pp. 2217-2222, 2001.
8. A. V. Kabashin, J.-P. Sylvestre, S. Patskovsky, M. Meunier, "Correlation between PL properties and morphology of of laser-ablated Si/SiO_x"*J. Appl. Phys.*, **91**, 3248, 2002.
9. M.Sendova-Vassileva, M.Tzenov, D.Dimova-Malinovska, M.Rosenbauer, M.Stutzmann, K.V.Josepovits, "Structural and luminescence studies of stain-etched and electrochemically etched germanium", *Thin Solid Films*, **255** (1995) 282
10. S.Miyazaki, K.Sakamoto, K.Shiba, M.Hirose, "Photoluminescence from anodized and thermally oxidized porous germanium ", *Thin Solid Films*, **255** (1995) 99
11. Y.Maeda, N.Tsukamoto, Y.Yazawa, Y.Kanemitsu, Y.Masumoto, "Visible photoluminescence of Ge microcrystals embedded in SiO_2 glassy matrices", *Appl.Phys.Lett.*, **59** (1991) 3168
12. L.Yue and Y.He, "Studies on room temperature characteristics and mechanism of visible luminescence of Ge-SiO_2 thin films", *J.Appl.Phys.*, **81** (1997) 2910
13. T.Kabayashi, T.Endoh, H.Fukada, S.Sakai, Y.Ueda, "Ge nanocrystals in SiO_2 films", *Appl.Phys.Lett.*, **71** (1997) 1195
14. L.Pavesi, L.Dal Negro, C.Mazzolenl, G.Franzo, and F.Priolo, "Optical gain in silicon nanocrystals ", *Nature*, **408** (2000) 440
15. V.S.-Y. Lin, K.Motesharei, K.P.S. Dancil, M.J.Sailor, and M.R.Ghadiri, "A porous silicon-based optical interferometric biosensor ", *Science*, **278** (1997) 840
16. R.E Hummel, S-S. Chang**, "**Novel technique for preparing porous silicon", *Appl. Phys. Lett.*, **61**, pp. 1965-1967, 1992.
17. E.F. Steigmeier, H. Auderset, B. Delley, and R. Morf, "Visible light emission from Si materials", *J. Luminescence*, **57,** pp. 9-12, 1993.
18. R.E. Hummel, A. Morrone, M. Ludwig, and S.-S. Chang, "On the origin of photoluminescence in spark-eroded (porous) silicon", *Appl. Phys. Lett.*, **63,** pp. 2771-2773, 1993.
19. M.H. Ludwig, A. Augustin, and R.E. Hummel, "Colour-switching effect of photoluminescent silicon after spark-processing in oxygen", *Semicond. Sci. Technol.*, **12,** pp. 981-986, 1997.

20. S.S.Chang, G.J.Choi, and R.E.Hummel, "Optical properties of spark-processed germanium", *Mat.Sci.Eng.*, **B 76** (2000) 237
21. A.V.Kabashin, M.Meunier, "Fabrication of photoluminescent Si-based layers by air optical breakdown near the silicon surface", *Appl.Surf.Sci.*, **186** (2002) 576.
22. A.V.Kabashin, M.Meunier, "Air optical breakdown on silicon as a novel method to fabricate photoluminescent Si-based nanostructures", *Proc. of SPIE*, **4636** (2002) 59.
23. S. Poulin, D.-Q. Yang, E. Sacher, C. Hyett, and T. H. Ellis, "The surface structure of Dow Cyclotene 3022, as determined by photoacoustic FTIR, confocal Raman and photoelectron spectroscopies", *Appl. Surf. Sci.*, **165** (2000) 24.
B. D. Cullity, *Elements of X-ray diffraction* (Addison-Westley, Reading, MA, 1978).
25. Yu.P. Raizer *Laser-Induced Discharge Phenomena* (Consultants Bureau, New York, 1977).